Supplementary Information

Robustness, Entrainment, and Hybridization in Dissipative Molecular Networks, and the Origin of Life

Brian J. Cafferty,[1] Albert S. Y. Wong,[1] Sergey N. Semenov,[1] Lee Belding,[1] Samira Gmür,[1] Wilhelm T. S. Huck,[2] and George M. Whitesides[1,3,4*]

[1] Department of Chemistry and Chemical Biology, Harvard University
12 Oxford Street, Cambridge, MA 02138

[2] Institute for Molecules and Materials, Radboud University Nijmegen, Heyendaalseweg 135, 6525 AJ Nijmegen, The Netherlands.

[3] Wyss Institute for Biologically Inspired Engineering, 60 Oxford Street, Cambridge, MA 02138

[4] Kalvi Institute for Bionano Science and Technology, Harvard University, 29 Oxford Street, Cambridge, MA 02138

Correspondence to: gwhitesides@gmwgroup.harvard.edu

Materials and Methods

Synthesis

General: All chemicals were obtained commercially and, unless stated, used without purification. Nuclear magnetic resonance (NMR) spectra were measured on a Varian INOVA I-500 spectrometer at 500 MHz for ^{1}H and 125 MHz for ^{13}C. The chemical shifts for ^{1}H and ^{13}C are given in parts per million (p.p.m.) relative to TMS, and calibrated using the residual 1H peak of the solvent; $\delta = 7.26$ for $CDCl_3$ and $\delta = 4.79$ for D_2O in ^{1}H NMR, and $\delta = 77.2$ for $CDCl_3$ in ^{13}C NMR.

N-Boc-L-alanine ethyl thioester: 3-dimethylaminopropyl-N'-ethylcarbodiimide hydrochloride (EDC·HCl) (2.8 g, 14.5 mmol) was added to a stirred solution of N-Boc-L-alanine (2 g, 10.6 mmol) and ethanethiol (1.2 mL, 23 mmol) in 15 mL of dimethylformamide (DMF) at 0˚C under an argon atmosphere. After allowing the reaction to proceed at 0 ˚C for one hour, the mixture was stirred at 20 ˚C overnight. DMF was removed in vacuo, and the residue was dissolved in ethyl acetate (EtOAc) and washed with water. The crude product was purified by flash chromatography (SiO_2, CH_2Cl_2 / EtOAc 95:5). Yield, 63% (2.3 g, 5.5 mmol). ^{1}H NMR: (500 MHz, $CDCl_3$) $\delta = 4.31$ (m, 1H), 2.87 (q, 2H), 1.45 (s, 9H), 1.37 (d, 3H), 1.25 (t, 3H).

Trifluoroacetic acid salt of L-alanine ethyl thioester: Trifluoroacetic acid (12 mL) was added dropwise to a solution of N-Boc-L-alanine thioester (1.25 g, 5.4 mmol) in dichloromethane (12 mL) stirring at 0˚C. The reaction was incubated at 0˚C for 15 minutes, and then at 20 ˚C for one hour. Solvents were removed in vacuo yielding a residue. The residue was dissolved in toluene followed by evaporation under vacuum. Co-evaporation with toluene was repeated until a white solid was obtained. Yield, 97% (1.3 g, 5.3 mmol). ^{1}H NMR: (500 MHz, $CDCl_3$), $\delta = 4.18$ (q,

1H), 2.85 (m, 2H), 1.43 (d, 3H), 1.11 (t, 3H). ^{13}C NMR: (125 MHz, $CDCl_3$), δ = 199.5, 55.0, 23.5, 16.5, 13.5.

N-Boc-L-glycine ethyl thioester: 3-dimethylaminopropyl-N'-ethylcarbodiimide hydrochloride (EDC·HCl) (3 g, 15.5 mmol) was added to a stirred solution of N-Boc-L-glycine (2 g, 11.4 mmol) and ethanethiol (1.5 mL, 28 mmol) in 12.5 mL of DMF at 0 ˚C under an argon atmosphere. After allowing the reaction to proceed at 0 ˚C for one hour, the mixture was stirred at 20 ˚C for 16 hours. DMF was removed in vacuo, and the residue was dissolved in EtOAc and washed with water. The crude product was purified by flash chromatography. (SiO_2, CH_2Cl_2 / EtOAc 95:5). Yield, 74 % (1.8 g, 8.3 mmol). ^1H NMR: (500 MHz, $CDCl_3$) δ = 4.04 (d, 1H), 2.91 (q, 2H), 1.46 (s, 9H), 1.26 (t, 3H).

Trifluoroacetic acid salt of L-glycine ethyl thioester: Trifluoroacetic acid (12 mL) was added dropwise to a solution of N-Boc-L-glycine thioester (1.08 g, 5.7 mmol) in dichloromethane (12 mL) stirring at 0 ˚C. The reaction was kept at 0 ˚C for 15 minutes, and then at 20 ˚C for one hour. Solvents were removed in vacuo yielding a residue. The residue was dissolved in DCM and a white powder was obtained from precipitation from diethyl ether. Yield, 98 % (0.98 g, 8.2 mmol). ^1H NMR: (500 MHz, $CDCl_3$) δ = 4.01 (s, 1H), 2.90 (q, 2H), 1.14 (t, 3H).

N-Boc-L-α-amino butyric acid ethyl thioester: 3-dimethylaminopropyl-N'-ethylcarbodiimide hydrochloride (EDC·HCl) (3 g, 15.5 mmol) was added to a stirred solution of N-Boc-L-α-amino butyric acid (2.7 g, 13.3 mmol) and ethanethiol (1.5 mL, 28 mmol) in 12.5 mL of DMF at 0 ˚C under an argon atmosphere. After allowing the reaction to proceed at 0 ˚C for one hour, the mixture was then stirred at 20 ˚C for 16 h. DMF was removed in vacuo, and the residue was dissolved in EtOAc and washed with water. The crude product was purified by flash chromatography. (SiO_2, CH_2Cl_2 / EtOAc 95:5). Yield, 68 % (2.24 g, 9.1 mmol). ^1H NMR:

(500 MHz, $CDCl_3$) δ = 4.28 (m, 1H), 2.86 (q, 2H), 1.88 (m, 2H), 1.45 (s, 9H), 1.23 (d, 3H), 0.94 (t, 3H).

Trifluoroacetic acid salt of L-α-aminobutyric acid ethyl thioester: Trifluoroacetic acid (12 mL) was added dropwise to a solution of N-Boc-L-α-amino butyric acid thioester (1.08 g, 5.7 mmol) in dichloromethane (12 mL) stirring at 0 ˚C. The reaction was kept at 0˚C for 15 minutes, and then at 20 ˚C for 1 hour. Solvents were removed in vacuo yielding a residue. The residue was dissolved in DCM and a white powder was obtained from precipitation from diethyl ether. Yield, 98 % (1.3 g, 8.3 mmol). ^{1}H NMR: (500 MHz, $CDCl_3$), δ = 4.12 (q, 1H), 2.86 (m, 2H), 1.87 (m, 2H), 1.12 (t, 3H), 0.86 (t, 3H).

Kinetics experiments

General: Kinetic experiments were performed at 25 °C in a 1 mL solution of 500 mM phosphate buffer (pH 7.5) in D_2O by monitoring the change in the ^{1}H NMR spectra. We calculated the progress of the reactions by integrating the ^{1}H NMR signal of the proton(s) linked to the α-carbon of the thioester and normalized this signal to that of an internal standard of 4,4-dimethyl-4-silapentane-1-sulfonic acid (DSS).

Determination of k_{hyd}, k_{aml} and k_{ncl} for AlaSEt, GlySEt and AbuSEt: The concentrations of the starting materials were calculated by setting the total integral of the α-protons equal to the starting concentration of thioester. For determination of the rate of hydrolysis (k_{hyd}) and the rate of aminolysis (k_{aml}) the starting concentration of reagent was 46 mM thioester. Only GlySEt was observed to undergo aminolysis, and all three thioesters were observed to undergo hydrolysis. For determination of the rate of native chemical ligation (k_{ncl}) the starting concentrations of reagents were 46 mM thioester and 46 mM sodium cystamine.

Determination of the initiation of the rate of auto-amplification: The rate of initiation of auto-amplification (the length of time of the lag phase before auto-amplification for reactions of cysteine and thioester) for mixtures of GlySEt and AbuSEt was compared to AlaSEt to determine ratios of AbuSEt and GlySEt that could be oscillatory. The rate of initiation of auto-amplification was determined by mixing each thioester alone at 46 mM with an equivalent of cystamine, and combinations of GlySEt and AbuSEt in which the total concentration of thioester was maintained at 46 mM. Spectra were acquired ever 72 seconds.

Reactions between GlySEt, AbuSEt and maleimide: To determine the thioester that reacted fastest with maleimide in a 1:1 mixture of GlySEt and AbuSEt, both thioesters were combined at 23 mM each with10 mM maleimide (the concentration of each compound used in the flow experiments). The concentrations of both amino acid amide products were determined by comparison to an internal standard (TSP). Spectra were acquired every 612 seconds.

Flow Experiments

Apparatus: For a detailed description of the micro-CSTR setup, please see reference 22. Briefly, a glass CSTR with a 250 μL volume and stir bar was imbedded in a polydimethylsiloxane (PDMS) base. The outflow of the CSTR was directed to a PDMS fast-in flow mixing chip used for derivatization of thiols with Elman's reagent, and a glass flow cell was coupled to a Cary 60 UV-vis spectrophotometer. Absorbance data was converted into total concentration of free thiol using calibration curves generated from known concentrations of ethanethiol in the reactor.

Oscillatory experiments: Four gas-tight syringes driven by syringe pumps were used for each experiment. Three syringes (numbered 1-3) were used to move reactants into and out of the CSTR. The volume of these syringes was either 2.5 mL or 5 mL depending on the amount of

time required for a given experiment. Syringe 1 contained the TFA salt of the thioester, or mixture of thioesters, dissolved in Milli-Q water at a concentration of 140 mM in total thioester. Syringe 2 contained cystamine hydrochloride at 276 mM in 3 M potassium phosphate solution buffered at pH 8. Syringe 3 contained maleimide at 31 mM and acrylamide at 962 mM dissolved in Milli-Q water. A fourth syringe that was 50 mL in volume was connected to the mixing chip, and supplied the Ellman's reagent, 5,5'-dithiobis-(2-nitrobenzoic acid (16.6mM) in a 2:3 mixture of MeOH:NaH_2PO_4 (208mM). Note that Ellman's reagent should be dissolved in MeOH before adding the solution of NaH_2PO_4. The flow rates for syringes 1-3 were the same and the flow rate for syringe 4 was nine times larger than that of syringes 1-3. Changing flow rates was automated using a Matlab program written in house.

Determination of the range of space velocity that produces stable oscillations. Syringe pumps were programed to control the flow rate of the syringes feeding the CSTR. For a typical experiment, each flow rate was monitored for 4-6 hours before the rate was increased. We initially tested ranges of flow rates for each mixture in order to determine which flow rates, if any, allowed the network to oscillate. If oscillations were observed, we repeated the experiments to define the range of space velocities where the oscillations can occur under the conditions tested. The UV-traces that formed from these experiments were processed to remove artifacts caused by air bubbles. Period of oscillation was determined by taking the average distance between all peaks at a given space velocity. The initial concentrations of starting material for all reactions: [thioester] = 46 mM, [cystamine] = 92 mM, [maleimide] = 10 mM, [acrylamide] = 320 mM, phosphate buffer (pH 8), 28 °C.

Simulations

Numerical Modeling

Numerical integrations were carried out using mathematical modelling comprising coupled nonlinear ordinary differential equations (ODEs). The ODEs describing the dynamics of the reaction network were obtained by deriving an equation for each of the species in the network using mass-action kinetics. These equations, implemented in MATLAB, are solved numerically in time using a standard integrator (ODE23t). The differential equations of the full model (shown below) were deduced from the reaction mechanisms (Table S1).

The rates of change in concentration of reactants and products are based on the consumption, production, and continuous in- and outflow of these molecules in the network using the following assumptions. i) Formation of ethanethiol (EtSH) from thioesters (RSEt) by hydrolysis (a first order reaction) and aminolysis (a second order reaction); which triggers auto-amplification. ii) Conjugate addition of thiols with maleimide (I_1) and acrylamide (I_2); an irreversible process that inhibits auto-amplification. iii) Disulfide exchange with thiols that has the forward reaction rate (*kss*); a reversible reaction required for auto-amplification. iv) The intramolecular step of the Kent ligation is assumed to occur instantaneously.

Table S1: Summary of proposed mechanisms and rate constants of the individual reactions in the CRN.

Individual reaction		Mechanism	Rate constant
Triggering step			
R1	Thioester hydrolysis:	RSEt +H_2O → R-OH + EtSH	$k_{hydr}^{(R)} = x\ h^{-1}$
R2	Thioester aminolysis:	2 RSEt → 2 EtSH + DKP	$k_{al}^{(R)} = y\ M^{-1}\ h^{-1}$
R3	Conjugate addition, EtSH and Maleimide:	EtSH + I_1 → EtS-I	$k_{inh}^{1} = 150\ M^{-1}\ h^{-1}$
Auto-activation step			
R4	Disulfide interchange, EtSH and CSSC:	EtSH + CSSC ↔ CSH + CSSEt	$k_{ss} = 0.444\ M^{-1}\ h^{-1}$
R5	Thiol-thioester interchange, RSEt and CSH (followed by an intramolecular Kent ligation):	RSEt + CSH ↔ [EtSH + RSC] → + RCSH	$k_l = 0.46\ M^{-1}\ h^{-1}$
R6	Disulfide interchange, RCSH and CSSC:	CSSC + RCSH ↔ RCSSC + CSH	$k_{ss} = 0.444\ M^{-1}\ h^{-1}$
Inhibition			
R7	Conjugate addition, EtSH and Acrylamide:	EtSH + I_2 → EtS-I_2	$k_{inh}^{2} = 0.145\ M^{-1}\ h^{-1}$
R8	Conjugate addition, CSH and Acrylamide:	CSH + I_2 → CS-I_2	k_{inh}^{2}
R9	Conjugate addition, RCSH and Acrylamide:	RCSH + I_2 → RCS-I_2	k_{inh}^{2}
Side reactions			
R10	Conjugate addition, CSH and Maleimide:	CSH + I_1 → CS-I_1	k_{inh}^{1}
R11	Conjugate addition, RCSH and Maleimide:	RCSH + I_1 → RCS-I_1	k_{inh}^{1}
R12	Disulfide interchange, CSSC and RCSH:	CSSC + RCSH ↔ RCSSC + CSH	k_{ss}
R13	Disulfide interchange, RCSSCR and EtSH:	RCSSCR + EtSH ↔ RCSSEt + RCSH	k_{ss}
R14	Disulfide interchange, EtSSEt and CSH:	EtSSEt + CSH ↔ EtSSC + EtSH	k_{ss}
R15	Disulfide interchange, RCSSC and EtSH:	RCSSC + EtSH ↔ RCSSEt + CSH	k_{ss}
R16	Disulfide interchange, RCSSC and EtSH:	RCSSC + EtSH ↔ EtSSC + RCSH	k_{ss}
R17	Disulfide interchange, RCSSC and AlaCSH:	RCSSC + RCSH ↔RCSSCR + CSH	k_{ss}
R18	Disulfide interchange, RCSSC and CSH:	RCSSC + CSH ↔ CSSC + AlaCSH	k_{ss}
R19	Disulfide interchange, EtSSEt and EtSH:	EtSSC + EtSH ↔ EtSSEt + CSH	k_{ss}
R20	Disulfide interchange, EtSSEt and CSH:	EtSSC + CSH ↔ CSSC + EtSH	k_{ss}
R21	Disulfide interchange, EtSSEt and AlaCSH:	EtSSC + RCSH ↔RCSSEt + CSH	k_{ss}
R22	Disulfide interchange, EtSSEt and AlaCSH:	EtSSC + RCSH ↔RCSSC + EtSH	k_{ss}

The set of rate equations describing the reaction network with a single thioester is based on seven key variables (concentration of reagents RSEt, CSSC, inhibitors I_1 and I_2, and thiol intermediates EtSH, CSH, RCSH) and the molecules that are formed through disulfide interchanges (RCSSC, RCSSEt RCSSCR, CSSEt, EtSSEt) are shown here. The substituent R = 1, 2, 3, … i.

Reagents:

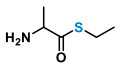
AlaSEt

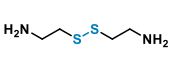
CSSC


I_1


I_2

$$\frac{d}{dt}RSEt = -\left(k_h^i + k_l^i[CSH] + k_{al}^i[RSEt]\right)[RSEt] + sv([RSEt]_0 - [RSEt])$$
$$\frac{d}{dt}CSSC = k_{ss}\left(([CSSEt] + [RCSSC])[CSH] - ([EtSH] + [RCSH])[CSSC]\right) + sv([CSSC]_0 - [CSSC])$$
$$\frac{d}{dt}I_1 = -k_{inh}^1([EtSH] + [CSH] + [RCSH])[I_1] + sv([I_1]_0 - [I_1])$$
$$\frac{d}{dt}I_2 = -k_{inh}^2([EtSH] + [CSH] + [RCSH])[I_2] + sv([I_2]_0 - [I_2])$$

Thiol Intermediates:


EtSH


CSH

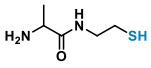
AlaCSH

$$\frac{d}{dt}EtSH = \left(k_h^i + k_l^i[CSH]\right)[RSEt] - (k_{inh}^1[I_1] + k_{inh}^2[I_2])[EtSH] - sv[EtSH]$$
$$+k_{ss}([CSH] + [RCSH])([CSSEt] + [RCSSEt] + [EtSSEt])$$
$$-k_{ss}([CSSC] + [RCSSC] + [CSSEt] + [RCSSEt] + [RCSSCR])[EtSH]$$

$$\frac{d}{dt}CSH = -\left(k_{inh}^1[I_1] + k_{inh}^2[I_2] + k_l^i[RSEt]\right)[CSH] - sv[CSH]$$
$$+k_{ss}\left(([CSSC] + [RCSSC] + [CSSEt])([EtSH] + [RCSH])\right)$$
$$-k_{ss}([RCSSC] + [CSSEt] + [RCSSCR] + [EtSSEt])[CSH]$$

$$\frac{d}{dt}RCSH = k_l[RSEt][CSH] - (k_{inh}^1[I_1] + k_{inh}^2[I_2])[RCSH] - sv[RCSH]$$
$$+k_{ss}([EtSH] + [CSH])([RCSSC] + [RCSSEt])$$
$$-k_{ss}([CSSC] + [RCSSC] + [CSSEt] + [RCSSEt] + EtSSEt)[RCSH]$$

Disulfide Intermediates:

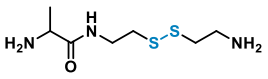
AlaCSSC

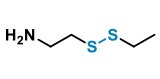
CSSEt

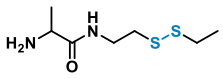
AlaCSSEt

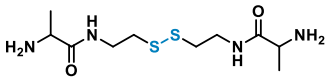
AlaCSSCAla

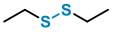
EtSSEt

$$\frac{d}{dt}RCSSC = k_{ss}\left(([CSSC] + [CSSEt])[RCSH] + ([RCSSEt] + [RCSSCR])[CSH]\right)$$
$$-k_{ss}([EtSH] + [CSH] + [RCSH])[RCSSC] - sv[RCSSC]$$

$$\frac{d}{dt}CSSEt = k_{ss}\left(([CSSC] + [RCSSC])[EtSH] + ([RCSSEt] + [EtSSEt])[CSH]\right)$$
$$-k_{ss}([EtSH] + [CSH] + [RCSH])[CSSCEt] - sv[CSSEt]$$

$$\frac{d}{dt}RCSSCR = k_{ss}\left(([RCSSEt] + [RCSSC])[RCSH] - ([CSH] + [EtSH])[RCSSCR]\right) - sv[RCSSCR]$$

$$\frac{d}{dt}EtSSEt = k_{ss}\left(([RCSSEt] + [CSSEt])[EtSH] - ([CSH] + [RCSH])[EtSSEt]\right) - sv[EtSSEt]$$
$$\frac{d}{dt}RCSSEt = k_{ss}\left(([CSSEt] + [EtSSEt])[RCSH] + ([RCSSCR] + [RCSSC])[EtSH] + ([EtSCCSEt] + [EtCSSC])[CSH]\right)$$
$$-k_{ss}([EtSH] + [CSH] + [RCSH])[CSSCEt] - sv[CSSEt]$$

The set of rate equations describing the reaction network with two or more thioesters based on eight key variables (concentration of reagents R_1SEt, R_2SEt CSSC, inhibitors I_1 and I_2, and thiol intermediates EtSH, CSH, RCSH) and the molecules that are formed through disulfide interchanges (RCSSC, RCSSEt RCSSCR, CSSEt, EtSSEt) are shown here.

Reagents:

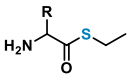

RSEt

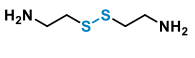

CSSC

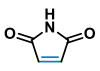

I_1

I_2

$$\frac{d}{dt}R_1SEt = -(k_h^1 + k_l^1[CSH])[R_1SEt] + sv([R_1SEt]_0 - [R_1SEt])$$
$$\frac{d}{dt}R_2SEt = -(k_h^2 + k_l^2[CSH] + k_{al}^2[R_2SEt])[R_2SEt] + sv([R_2SEt]_0 - [R_2SEt])$$
$$\frac{d}{dt}CSSC = k_{ss}(([CSSEt] + [RCSSC])[CSH] - ([EtSH] + [RCSH])[CSSC]) + sv([CSSC]_0 - [CSSC])$$
$$\frac{d}{dt}I_1 = -k_{inh}^1([EtSH] + [CSH] + [RCSH])[I_1] + sv([I_1]_0 - [I_1])$$
$$\frac{d}{dt}I_2 = -k_{inh}^2([EtSH] + [CSH] + [RCSH])[I_2] + sv([I_2]_0 - [I_2])$$

Thiol Intermediates:

EtSH

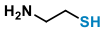

CSH

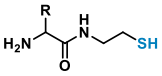

RCSH

$$\frac{d}{dt}EtSH = (k_h^1 + k_l^1[CSH] + k_{al}^1[R_1SEt])[R_1SEt] + (k_h^2 + k_l^2[CSH] + k_{al}^2[R_2SEt])[R_2SEt] - (k_{inh}^1[I_1] + k_{inh}^2[I_2])[EtSH] - sv[EtSH]$$
$$+k_{ss}([CSH] + [RCSH])([CSSEt] + [RCSSEt] + [EtSSEt])$$
$$-k_{ss}([CSSC] + [RCSSC] + [CSSEt] + [RCSSEt] + [RCSSCR])[EtSH]$$
$$\frac{d}{dt}CSH = -(k_{inh}^1[I_1] + k_{inh}^2[I_2] + k_l^1[R_1SEt] + k_{al}^2[R_2SEt])[CSH] - sv[CSH]$$
$$+k_{ss}(([CSSC] + [RCSSC] + [CSSEt])([EtSH] + [RCSH]))$$
$$-k_{ss}([RCSSC] + [CSSEt] + [RCSSCR] + [EtSSEt])[CSH]$$
$$\frac{d}{dt}RCSH = (k_l^1[R_1SEt] + k_{al}^2[R_2SEt])[CSH] - (k_{inh}^1[I_1] + k_{inh}^2[I_2])[RCSH] - sv[RCSH]$$
$$+k_{ss}([EtSH] + [CSH])([RCSSC] + [RCSSEt])$$
$$-k_{ss}([CSSC] + [RCSSC] + [CSSEt] + [RCSSEt] + EtSSEt)[RCSH]$$

Disulfide Intermediates:

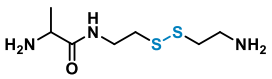

RCSSC

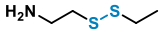

CSSEt

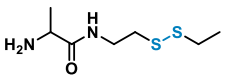

RCSSEt

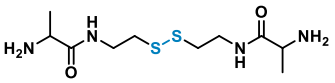

RCSSCR

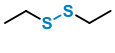

EtSSEt

$$\frac{d}{dt}RCSSC = k_{ss}(([CSSC] + [CSSEt])[RCSH] + ([RCSSEt] + [RCSSCR])[CSH])$$
$$-k_{ss}([EtSH] + [CSH] + [RCSH])[RCSSC] - sv[RCSSC]$$
$$\frac{d}{dt}CSSEt = k_{ss}(([CSSC] + [RCSSC])[EtSH] + ([RCSSEt] + [EtSSEt])[CSH])$$
$$-k_{ss}([EtSH] + [CSH] + [RCSH])[CSSCEt] - sv[CSSEt]$$
$$\frac{d}{dt}RCSSCR = k_{ss}(([RCSSEt] + [RCSSC])[RCSH] - ([CSH] + [EtSH])[RCSSCR]) - sv[RCSSCR]$$
$$\frac{d}{dt}EtSSEt = k_{ss}(([RCSSEt] + [CSSEt])[EtSH] - ([CSH] + [RCSH])[EtSSEt]) - sv[EtSSEt]$$
$$\frac{d}{dt}RCSSEt = k_{ss}(([CSSEt] + [EtSSEt])[RCSH] + ([RCSSCR] + [RCSSC])[EtSH] + ([EtSCCSEt] + [EtCSSC])[CSH])$$
$$-k_{ss}([EtSH] + [CSH] + [RCSH])[CSSCEt] - sv[CSSEt]$$

Analysis of oscillations: Our mathematical model can also predict regimes in which oscillations can occur. We have developed two scripts (*phase plot generator*, and a *wave classifier*) to analyze the key characteristics of the network (such as the amplitude and the frequency or period of oscillation). We used the *phase plot generator* to screen combinations of parameters.

Function: $\text{phase plot generator}(p, q, \dots) = \text{amp}, \text{per of oscillations},$

where parameter $p = \begin{pmatrix} p_1 \\ p_2 \\ \vdots \\ p_n \end{pmatrix}$, and parameter $q = (q_1, q_2, \cdots, q_n)$

In more detail, simulated time series (typically ~10^4), each with a different combination of p and q, are merged into a temporary file. Subsequently, the time series (simulated by either the set of ODEs for networks with a single thioester, or the set for networks with more than one thioester) are examined by the *wave classifier algorithm*. We used this procedure to assess the network function by searching for local maximum-minimum-maximum (mmm) patterns in the time traces of thiols (i.e., EtSH + CSH + RCSH). The overall response is considered a *sustained oscillation* when at least three consecutive mmm patterns have the same values (within a defined confidence interval) as their left and right neighbors, with validity tested by the criterion:

$|([\text{Thiols}]_{\max 1} - [\text{Thiols}]_{\min}) - |[\text{Thiols}]_{\min} - [\text{Thiolsr}]_{\max 2}|| < \text{p}([\text{Thiols}]_{\max 1} - [\text{Thiols}]_{\min})$, where $\text{p} = 0.003$.

The absence of a mmm pattern, or a pattern that show differences in at least one neighbor is classified as *no sustained oscillation*. If oscillations exist, the script records the amplitude and the periodicity of the oscillations. Finally, the *phase plot generator* projects the screening results as a phase plot showing both the occurrence of the network function and its characteristics.

Output: of the generator heatmap $= \begin{pmatrix} \text{per}(p_1, q_1) & \cdots & \text{per}(p_1, q_n) \\ \vdots & \ddots & \vdots \\ \text{per}(p_n, q_1) & \cdots & \text{per}(p_n, q_n) \end{pmatrix}$

Linear stability analysis of the four-component model of the mixed oscillator

The oscillator model can be reduced to a four-component model by applying three approximations: first, that both positive feedback loops are described by simple quadratic autocatalysis with rate constants k_{11} and k_{12}; second, that the negative feedback loop (reaction with acrylamide) is described by a first-order reaction with rate constant k_3; and third, that the end products can be neglected.

With these assumptions, the system of reactions is described by:

$$S_1 + A \xrightarrow{k_{11}} 2A$$
$$S_2 + A \xrightarrow{k_{12}} 2A$$
$$S_1 \xrightarrow{k_{41}} A$$
$$S_2 \xrightarrow{k_{42}} A$$
$$S_2 + S_2 \xrightarrow{k_5} 2A$$
$$I + A \xrightarrow{k_2} \otimes$$
$$A \xrightarrow{k_3} \otimes$$
$$A \xrightarrow{k_0} \otimes$$
$$I \xrightarrow{k_0} \otimes$$
$$S_1 \xrightarrow{k_0} \otimes$$
$$S_2 \xrightarrow{k_0} \otimes$$
$$\xrightarrow{k_0 I_0} I$$
$$\xrightarrow{k_0 S_{01}} S_1$$
$$\xrightarrow{k_0 S_{02}} S_2$$

Where A represents [EtSH] + [AlaNHCH$_2$CH$_2$SH] + [GlyNHCH$_2$CH$_2$SH] + [CSH]; I represents [Maleimide]; S_1 represents [AlaSEt]; S_2 represents [GlySEt]; $k_{1\text{-}5}$ are rate constants; and k_0 is space velocity; $\otimes$ indicates washout or for the formation of inactive products. The system of kinetic equations takes the following form:

$$dA/dt = k_{11}S_1A + k_{12}S_2A - k_2IA - k_3A - k_0A + k_{41}S_1 + k_{42}S_2 + k_5S_2^2$$

$$dI/dt = k_0I_0 - k_0I - k_2IA$$

$$dS_1/dt = k_0S_{01} - k_0S_1 - k_{41}S_1 - k_{11}S_1A$$

$$dS_2/dt = k_0S_{02} - k_0S_2 - k_{42}S_2 - k_{12}S_2A - k_5S_2^2$$

To represent the experimental system, we used the following values:

I_0 = 0.01 M, k_{11} = 0.25 $s^{-1}M^{-1}$, k_{12} = 0.8 $s^{-1}M^{-1}$, k_2 = 300 $s^{-1}M^{-1}$, k_3 = 0.0055 s^{-1}, k_{41} = $8\cdot10^{-5}$ s^{-1}.

k_{42} = $9\cdot10^{-5}$ s^{-1}. k_5 = 0.0306 $s^{-1}M^{-1}$

S_{01} and S_{02} were chosen based on the specific mixtures of thioesters.

The steady-states are defined by:

$$\frac{(k_{12}A + k_{42})\cdot(\sqrt{(k_0 + k_{42} + k_{12}A)^2 + 4k_5k_0S_{02}} - (k_0 + k_{42} + k_{12}A))}{2k_5} - \frac{k_2k_0I_0A}{k_0 + k_2A} - (k_0 + k_3)A +$$
$$\frac{(\sqrt{(k_0 + k_{42} + k_{12}A)^2 + 4k_5k_0S_{02}} - (k_0 + k_{42} + k_{12}A))^2}{4k_5} + \frac{k_{11}k_0S_{01}A}{k_0 + k_{41} + k_{11}A} + \frac{k_{41}k_0S_{01}}{k_0 + k_{41} + k_{11}A} = 0$$

To analyze the stability of the steady-states we used the Jacobian matrix (**J**), and determine the eigenvalues (λ) such that the following is not invertible:

$$\begin{matrix} k_{11}S_1 + k_{11}S_1 - k_2I - k_3 - k_0 - \lambda & -k_2A & k_{11}A + k_{41} & k_{12}A + 2k_5S_2 + k_{42} \\ -k_2I & -k_0 - k_2A - \lambda & 0 & 0 \\ -k_{11}S_1 & 0 & -k_{11}A - k_0 - k_{41} - \lambda & 0 \\ -k_{21}S_2 & 0 & 0 & -k_{12}A - 2k_5S_2 - k_{42} - k_0 - \lambda \end{matrix}$$

We used a Mathematica script to compute and plot the steady states and their stability.

Supplementary Discussions

Numerical simulations: Because the rate of formation of ethanethiol during the triggering step is significantly different for AlaSEt and GlySEt (Figure 2 in main text), we examined the influence of two competing processes that control the formation and consumption of ethanethiol as a function of space velocity. Increasing the space velocity of a network over the range where it oscillates stably will: i) increase the rate of addition of maleimide to the reactor (Figure S8), which increases the length of the triggering step ($t_{triggering} \propto k_0$[maleimide], where k_0 is space velocity); and ii) increase in the rate of addition of the thioesters to the reactor, which increases the rate of formation of ethanethiol and decreases the length of the triggering step ($t_{triggering} \propto 1/k_0$[thioesters]). For an oscillatory network to form, the rate of formation of ethanethiol must be, at some point, larger than the rate of addition of maleimide to the reactor during the triggering step. When space velocity is increased above the range where the network oscillates stably, the network will transition into a steady state, because the rate of addition of maleimide to the reactor will be greater than the rate of formation of ethanethiol.

Networks with AlaSEt and GlySEt can compensate for changes in space velocity and oscillate over a larger range of space velocity than the network with AlaSEt alone. We analyzed the influence of space velocity on the rate of formation of ethanethiol. Figure S8 shows an example of how the rate of formation of ethanethiol changes for each thioester separately (and combined) as a function of space velocity at the end of the triggering step (and just prior to auto-amplification) in the network with a different value of χ_{GlySEt} (0.2, 0.3, 0.35, and 0.4). As the value of χ_{GlySEt} increases, GlySEt makes a more significant contribution to the formation of

ethanethiol. Networks with χ_{GlySEt} of 0.35 and 0.4 have rates of formation of ethanethiol that is dominated by GlySEt at larger space velocity, and dominated by AlaSEt at smaller space velocity. For example, Figure S9c shows an example of how the rate of formation of ethanethiol changes for the network with χ_{GlySEt} = 0.35. The rate of ethanethiol formed by AlaSEt is larger than GlySEt at space velocities below 2.5 x 10^{-2} min^{-1}, but smaller than GlySEt at space velocities above 2.5 x 10^{-2} min^{-1}. Thus, at these molar ratios the network can dynamically compensate for changes in its environment through a cooperative process where the thioesters switch 'roles'.

The plot in Figure S10 shows that the period of oscillation decreases as k_{hyd} increases. The decrease in the sensitivity of the period of oscillation to changes in space velocity for the network with AlaSEt and GlySEt compared to the network with AlaSEt alone can be understood to result from two opposing factors i) increasing space velocity increases the period of oscillation (Figure 5a shows that networks with thioesters that have larger values of k_{hyd} oscillate at larger space velocities), and ii) increasing the rate of formation of ethanethiol decreases the period of oscillation. Because rate of formation of ethanethiol by GlySEt increases more than the rate produced by AlaSEt, networks with both GlySEt and AlaSEt can compensate for changes in space velocity, and thus maintain a more consistent period of oscillation, better than networks with AlaSEt alone.

Linear stability analysis: A bifurcation represents a set of conditions for which a smooth change in a control parameter causes a sudden shift in the behavior of the network. To explain the nature of the bifurcation between oscillatory and steady state behavior at low and high limiting space velocities for the heterogeneous network, we performed linear stability analysis on a simple four variable kinetic model (see description of the model above). For the network with

AlaSEt alone, as space velocity increases, two bifurcations are observed (*23*). The network initially transitions from a steady state to sustained oscillations through an Hopf bifurcation (marking the lower limit of oscillation). As the space velocity increases further, the oscillatory network transitions to a stable steady state through a Fold bifurcation (marking the upper limit of oscillation).

Linear stability analysis and numerical modeling show that the Hopf bifurcation is different for the mixed network as it does not mark the lower limit of oscillation. For the heterogeneous network with different mole fractions of GlySEt, a locally stable steady state and sustained oscillations were observed to coexist at space velocities below the Hopf bifurcation (Figure S11). This result suggests that at these space velocities (i.e., space velocities that are immediately adjacent to the Hopf bifurcation) the network is bistable; meaning that the network can exist in either an oscillatory state or a steady state. The range of space velocities that have this property increases with increasing χ_{GlySEt}. At this bistable region, the network behavior (steady state, oscillation) is determined by the initial conditions of the network. For example, if initial starting conditions are far from steady state conditions (e.g., if the initial concentration of thiol in the reactor is 0 and no thioester has been consumed), an oscillatory network will be favored (Figure S12a). If, however, the initial starting conditions are within an attractor of the steady state (e.g., if the initial concentrations are close to steady state concentrations) a network with steady-state behavior will be favored (Figure S12b). This characteristic of heterogeneous networks makes them robust as they are able to oscillate at values of space velocity that are below the Hopf bifurcation. Specifically, the oscillatory network is more robust to *changes* in space velocity, as it will be able to adapt to changes (potentially resulting from a noisy

environment) that lead to space velocities that are less than those at the Hopf bifurcation, which networks with a single thioester alone cannot do.

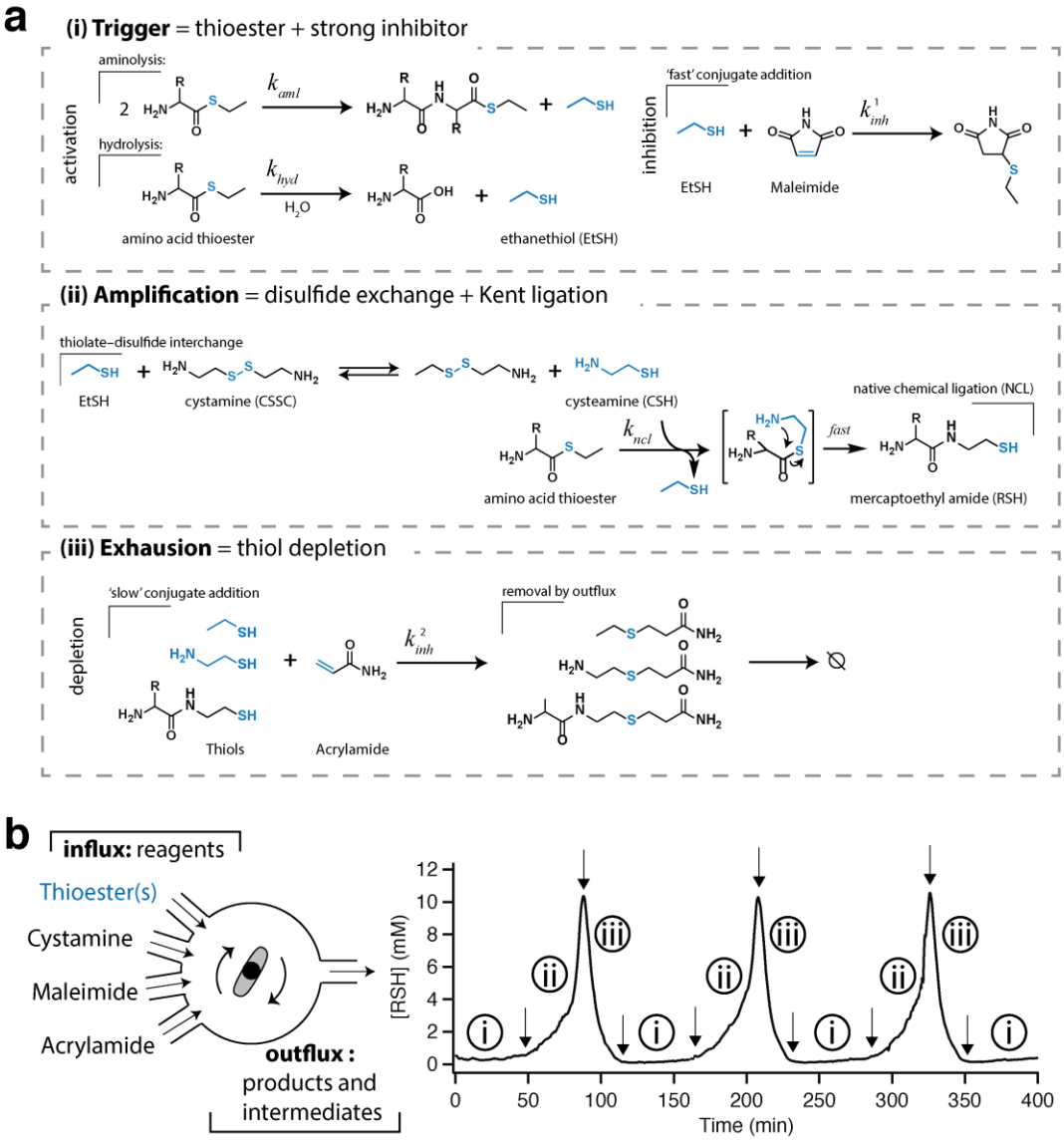

Figure S1. (**a**) Detailed reaction scheme of the oscillating network based on three chemical processes: (i) triggering, (ii) amplification, (iii) exhaustion. The formation of ethanethiol in the

triggering step occurs either through hydrolysis (k_{hyd}), or through aminolysis (k_{aml}). The formation of mercaptoethyl amide in the amplification step occurs through native chemical ligation (k_{ncl}). (**b**) The CSTR is fed with thioester(s) and other components (cystamine, maleimide, and acrylamide) to create an oscillating network in thiols (RSH). The three chemical steps are indicated by 1, 2, and 3.

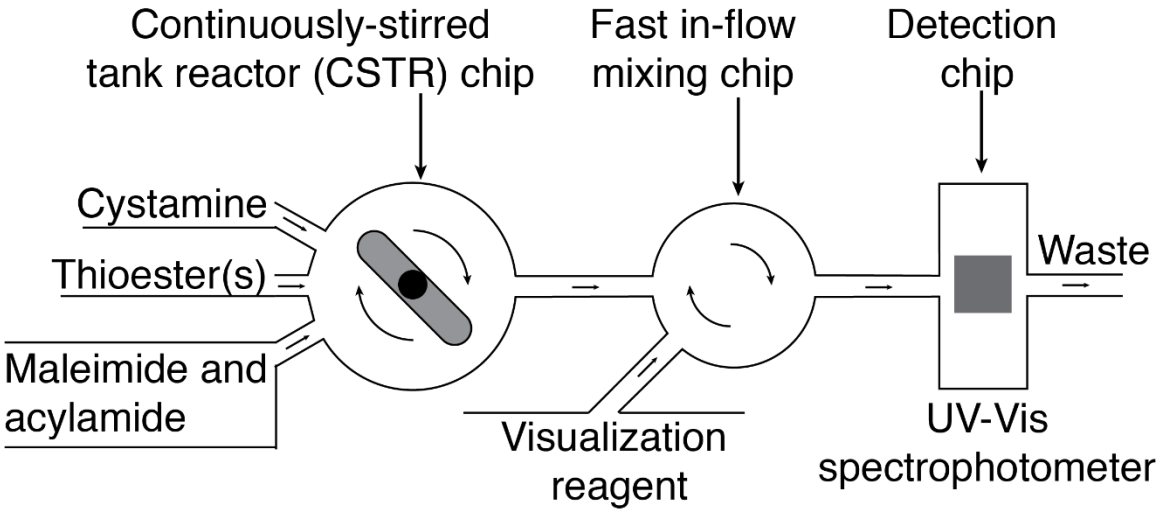

Figure S2. Schematic representation of the continuous stirred-tank reactor (CSTR). In this apparatus, syringe pumps feed reactants to the inlet ports of the CSTR. For continuous sampling, a tube connected to the outlet port of the CSTR takes the effluent (products and reactants) to a fast in-flow mixing detection chip.

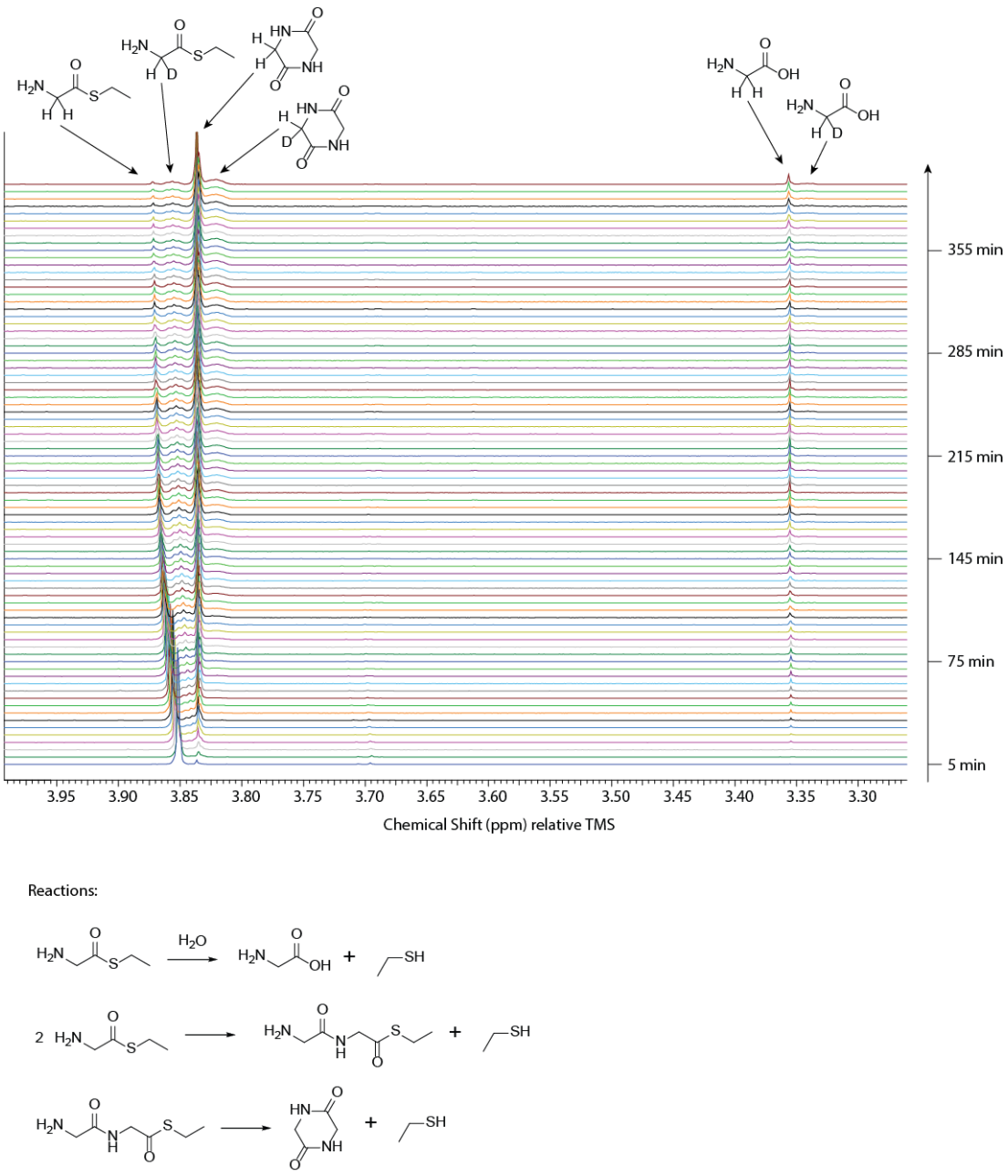

Figure S3. ^{1}H NMR analysis of hydrolysis and aminolysis of GlySEt in D_2O. Chemical structures of GlySEt, diketopiperizine (the aminolysis product), and glycine are labeled above the corresponding proton resonances. The individual reactions are displayed below the plot. Reaction conditions: 500 mM phosphate buffer pH 7.5, 25 °C, D_2O, [GlySEt] = 46 mM.

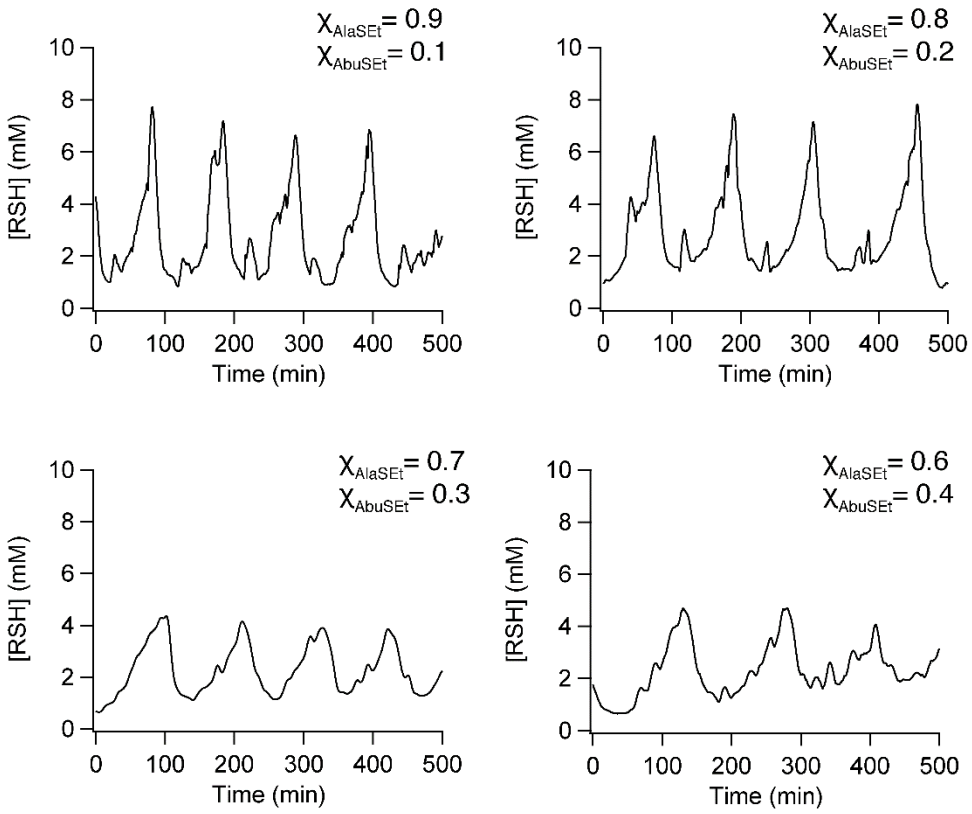

Figure S4. Experimental data from reactions containing different mole fractions of AlaSEt and AbuSEt (listed above each plot), cystamine, maleimide and acrylamide at the same space velocity (1.2×10^{-2} min^{-1}). Reaction conditions: 1 M potassium phosphate buffer pH 8.0, [AlaSEt] + [AbuSEt] = 46 mM, [cystamine] = 92 mM, [maleimide] = 10 mM, [acrylamide] = 320 mM, 28 °C.

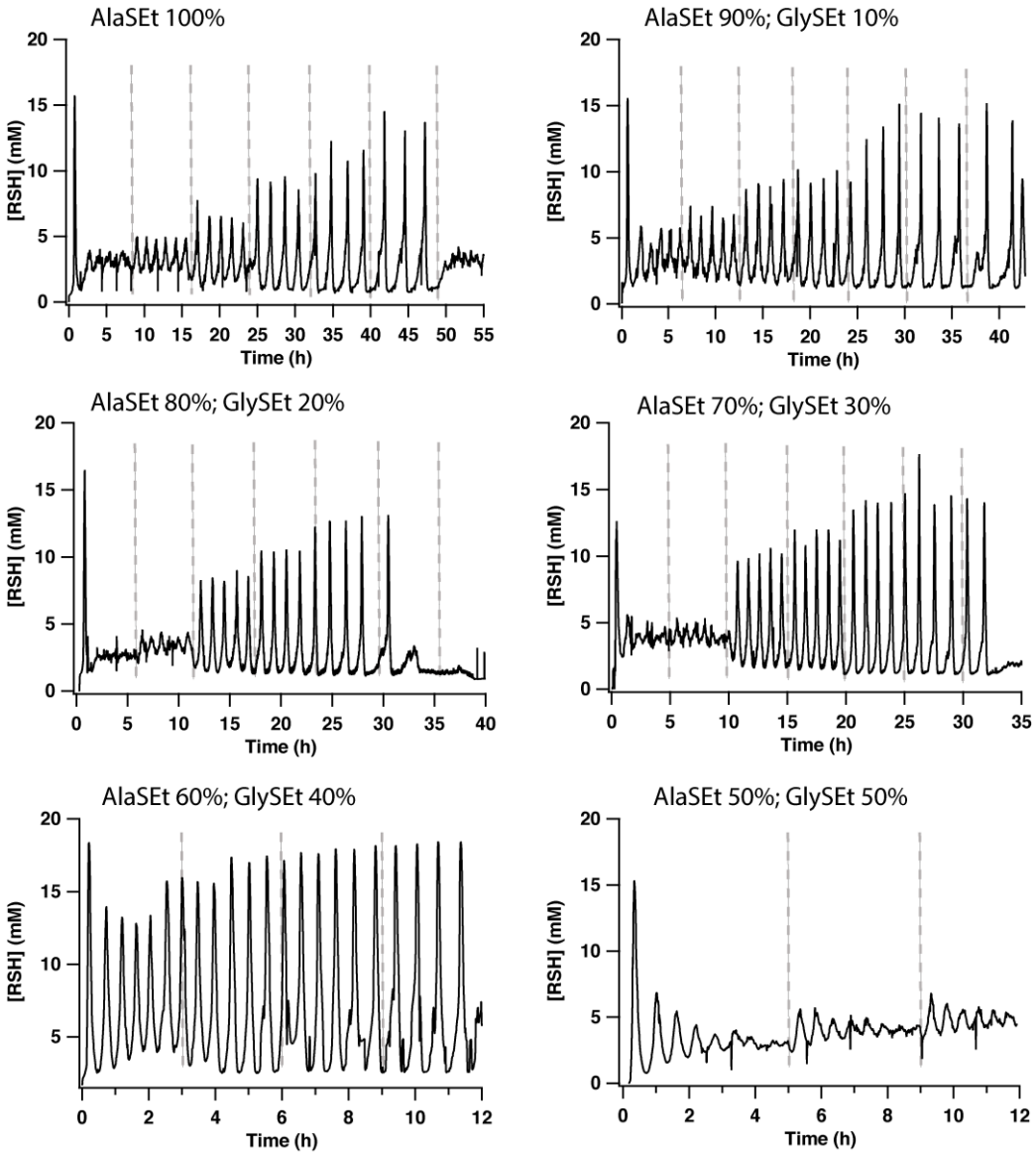

Figure S5. Experimental data from reactions containing different percentages of AlaSEt and GlySet (listed above each plot), cystamine, maleimide and acrylamide at different space velocities. Dashed grey lines indicate the time when the space velocity was increased and corresponds to space velocities shown in Figure 4c. Reaction coniditions: 1 M potassium phosphate buffer pH 8.0, [AlaSEt] + [GlySEt] = 46 mM, [cystamine] = 92 mM, [maleimide] = 10 mM, [acrylamide] = 320 mM, 28 °C.

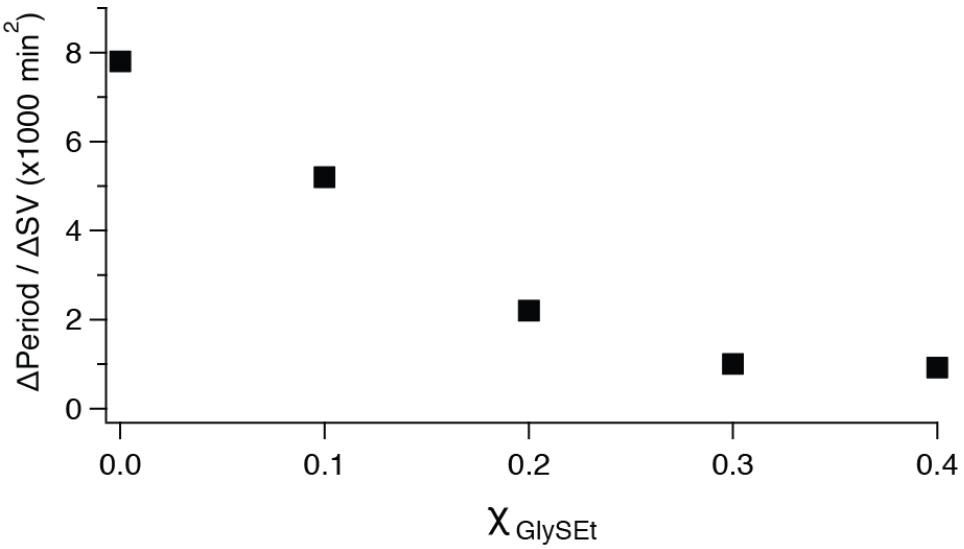

Figure S6. Plot of the change in period as a function of the change in space velocity from the linear fits in Figure 4c. The plot shows the influence of the mole fraction (χ_{GlySEt}) on the sensitivity of the frequency of oscillation to change in space velocity.

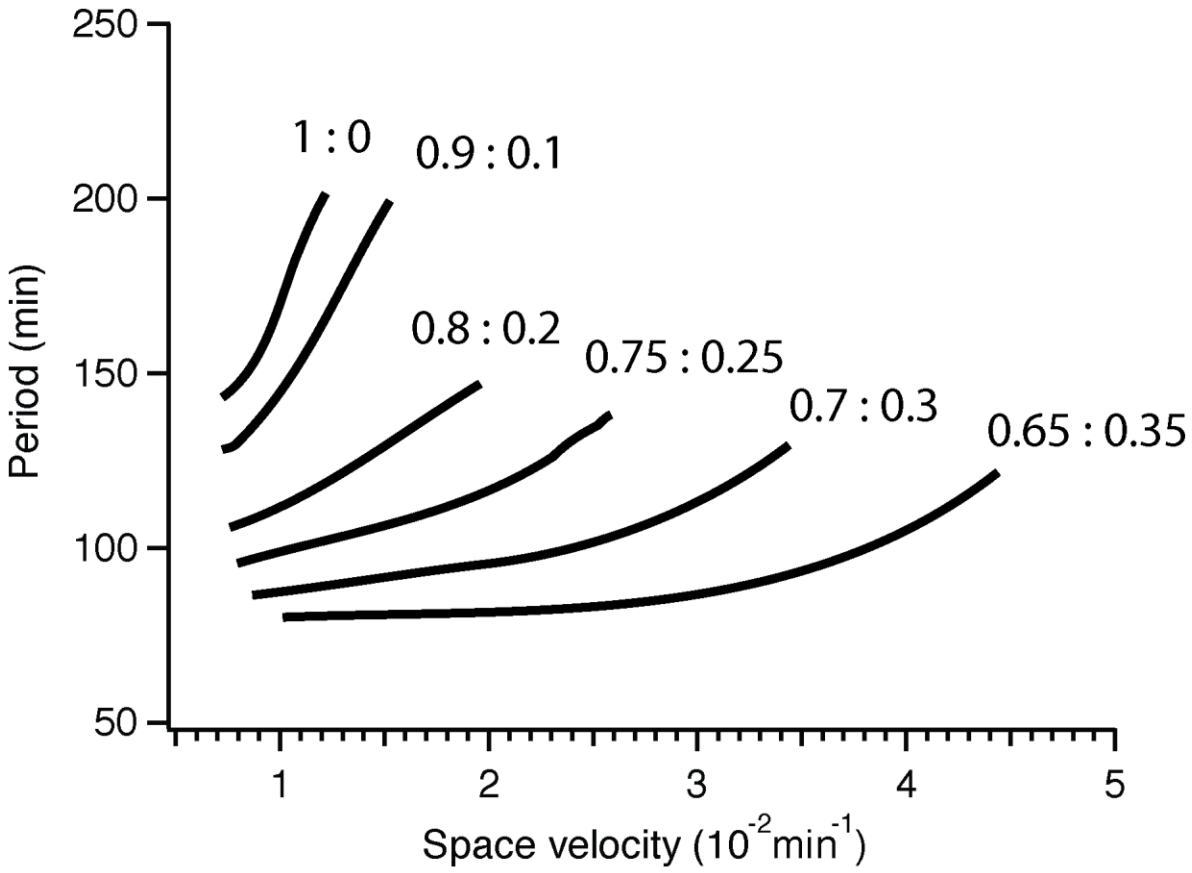

Figure S7. Plot showing the effect of space velocity on the stability and period of oscillation for networks with different values of χ_{GlySEt} and χ_{AlaSEt} (the ratio of AlaSEt to GlySEt for each simulation are listed above the corresponding trace). Simulations were performed with initial concentrations of [thioester] = 46 mM, [cystamine] = 92 mM, [maleimide] = 10 mM, [acrylamide] = 320 mM.

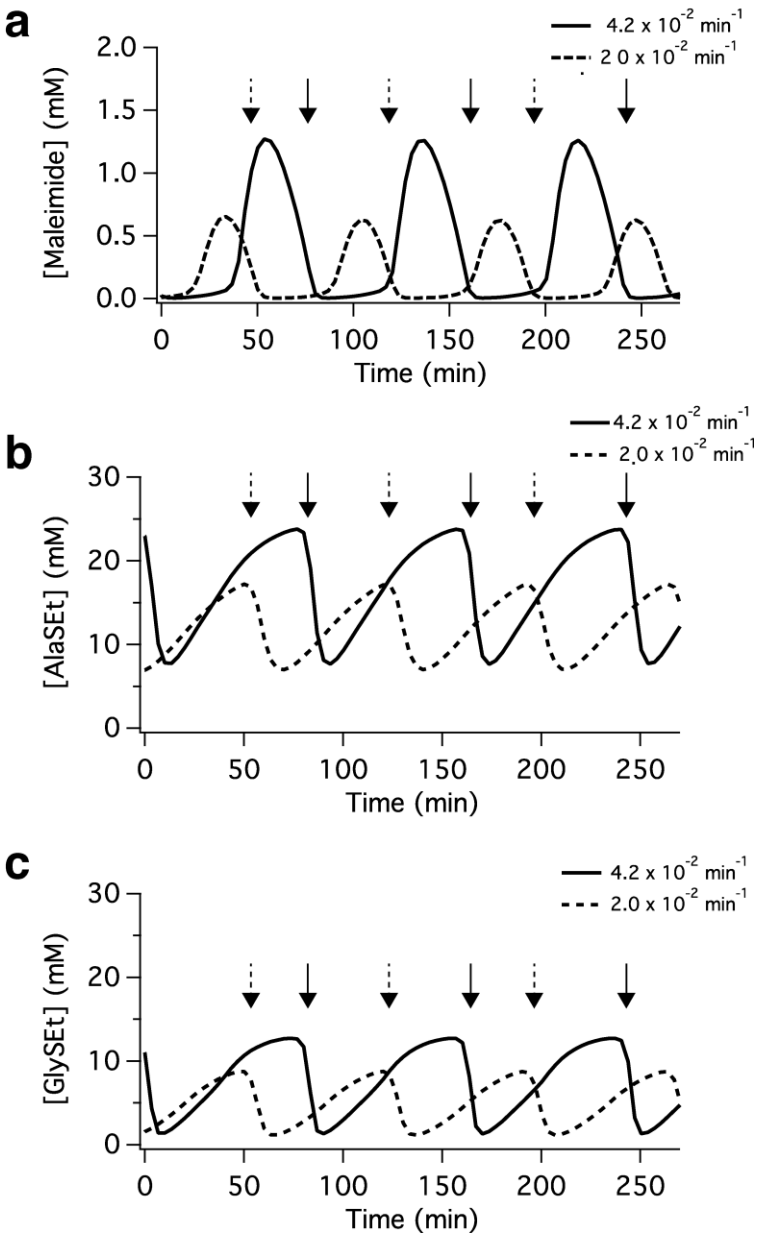

Figure S8. Influence of space velocity on the concentration of (**a**) maleimide, (**b**) AlaSEt, and (**c**) GlySEt in a network that contained a ratio of AlaSEt to GlySEt of 6:4. The simulations were performed at two space velocities, 4.2×10^{-2} min^{-1} and 2.0×10^{-2} min^{-1}. See list of ordinary differential equations used for modeling above. Arrows indicate time points when the network transitioned to the auto-amplification step, solid lines for the space velocity of 4.2×10^{-2} min^{-1} and dashed lines for the space velocity of 2.0×10^{-2} min^{-1}.

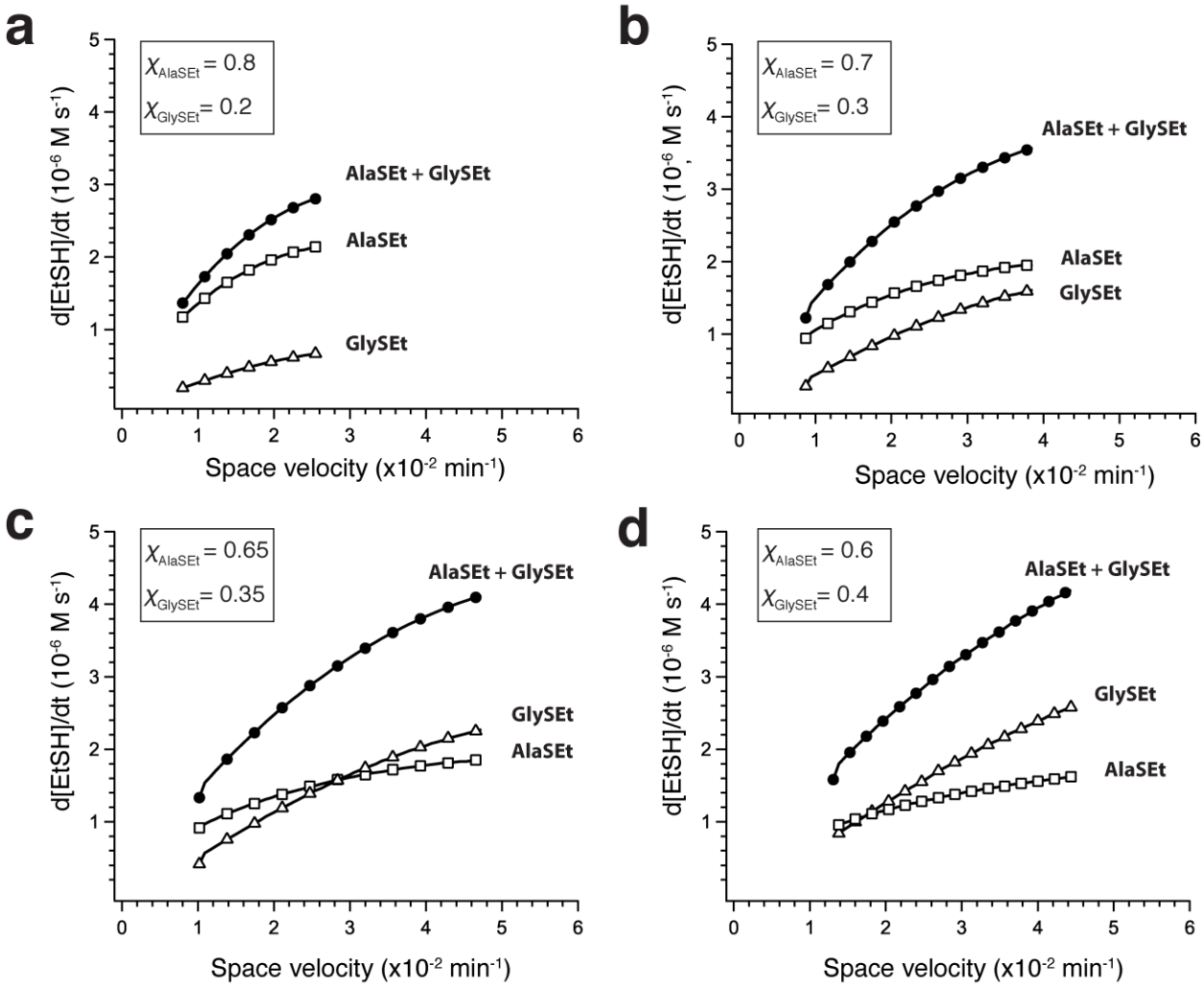

Figure S9. Influence of space velocity on the rate of formation of ethanethiol from aminolysis of GlySEt (open triangles) and hydrolysis of AlaSEt (open squares) together with the summed rate of formation of ethanethiol (filled circles) at the end of the triggering step for networks with (**a**) χ_{GlySEt} = 0.2 and $\chi_{AlaSEtt}$ = 0.8, (**b**) χ_{GlySEt} = 0.3 and $\chi_{AlaSEtt}$ = 0.7, (**c**) χ_{GlySEt} = 0.35 and $\chi_{AlaSEtt}$ = 0.65, and (**d**) χ_{GlySEt} = 0.4 and $\chi_{AlaSEtt}$ = 0.6.

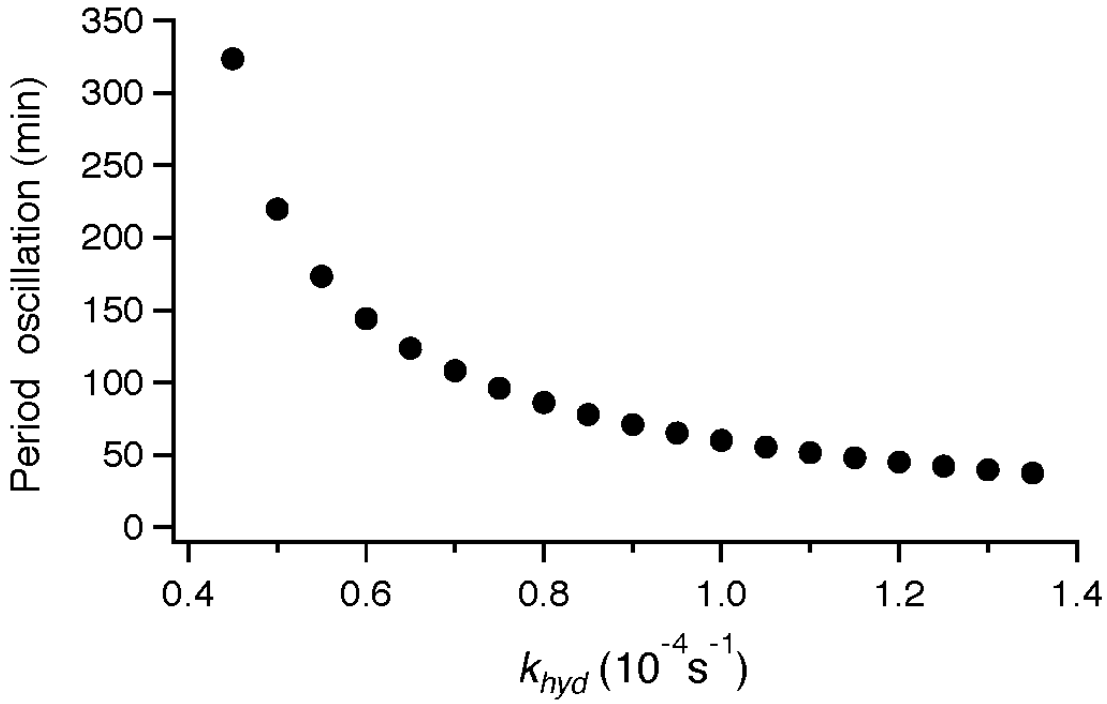

Figure S10. Influence of the value of k_{hyd} on the period of oscillation. The space velocity for each simulation was constant at 1.2×10^{-2} min^{-1} and initial concentrations were [Thioester] = 46 mM, [Mal] = 10 mM. These simulations were performed for networks with only one thioester that forms ethanethiol through hydrolysis alone but with different values of $k_{hyd.}$

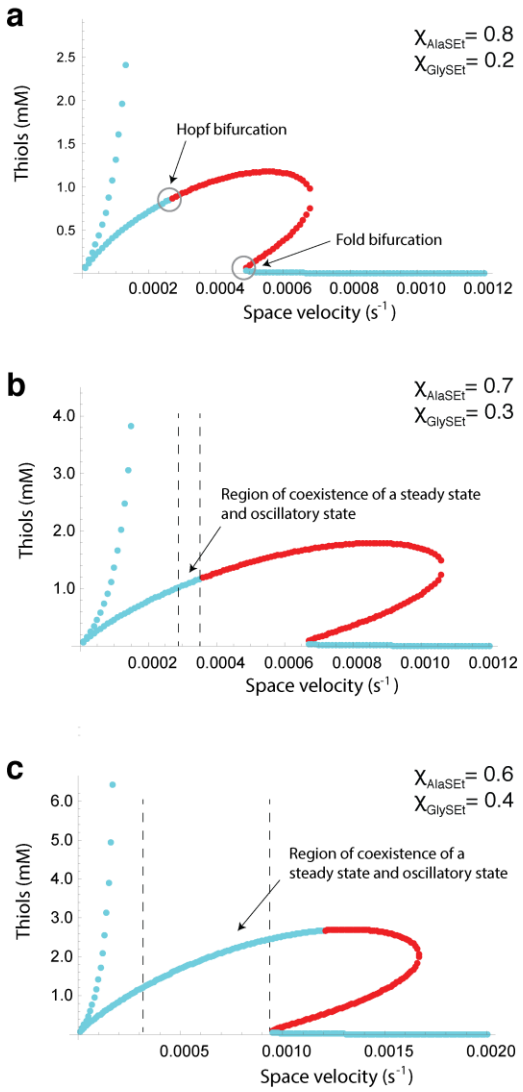

Figure S11. Results from linear stability analysis of mixtures of AlaSEt and GlySEt. Blue points represent stable steady states and red points represent unstable steady states. Mole fraction of AlaSEt to GlySEt examined were (**a**) 0.8:0.2, (**b**) 0.7:0.3, and (**c**) 0.6:0.4. We determined the area of coexistence of a steady state and sustained oscillations through numerical integration of the equations of the four-variable model. Specifically, we integrated the equations with initial conditions $[A_0] = 0$; $[I_0] = 0.01$ M; $[S1_0] = S_{01}$; $[S2_0] = S_{02}$ and considered that a region of the parameter space contains a stable orbit if we observe sustained oscillations with these initial

conditions for 500 hours. For an example of coexistence of a locally stable steady state and sustained oscillations see Figure S12.

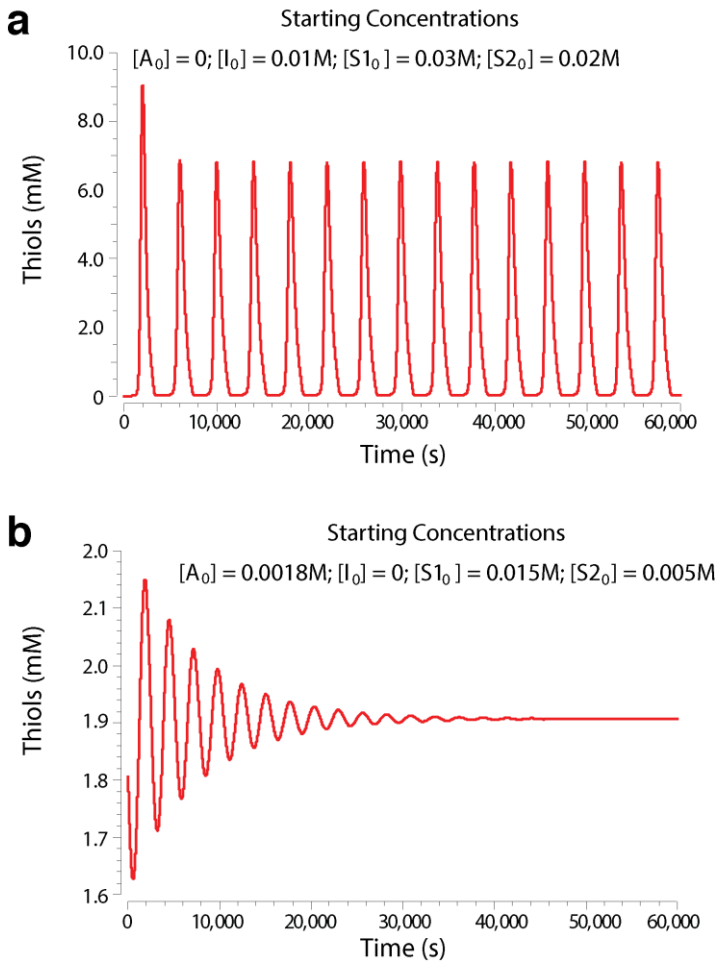

Figure S12. Coexistence of a locally stable steady state and sustained oscillations in the four-variable model of the thiol oscillator with AlaSEt and GlySEt ($\chi_{AlaSEt} = 0.6$; $\chi_{GlySEt} = 0.4$). Both plots (**a** and **b**) were obtained from the same model ($I_0 = 0.01$ M, $S_{01} = 0.03$ M, $S_{02} = 0.02$ M, $k_0 = 0.0006$ s^{-1}, $k_{11} = 0.25$ $s^{-1}M^{-1}$, $k_{12} = 0.8$ $s^{-1}M^{-1}$, $k_2 = 300$ $s^{-1}M^{-1}$, $k_3 = 0.0055$ s^{-1}, $k_{41} = 8 \cdot 10^{-5}$ s^{-1}. $k_{42} = 9 \cdot 10^{-5}$ s^{-1}. $k_5 = 0.0306$ $s^{-1}M^{-1}$) but with different initial conditions. Initial conditions in **a** are far from steady state values and conditions in **b** are close to steady state values ($A_{SS} = 0.00191$ M, $I_{SS} = 1 \cdot 10^{-5}$ M, $S1_{SS} = 0.0156$ M, $S2_{SS} = 0.0051$ M).

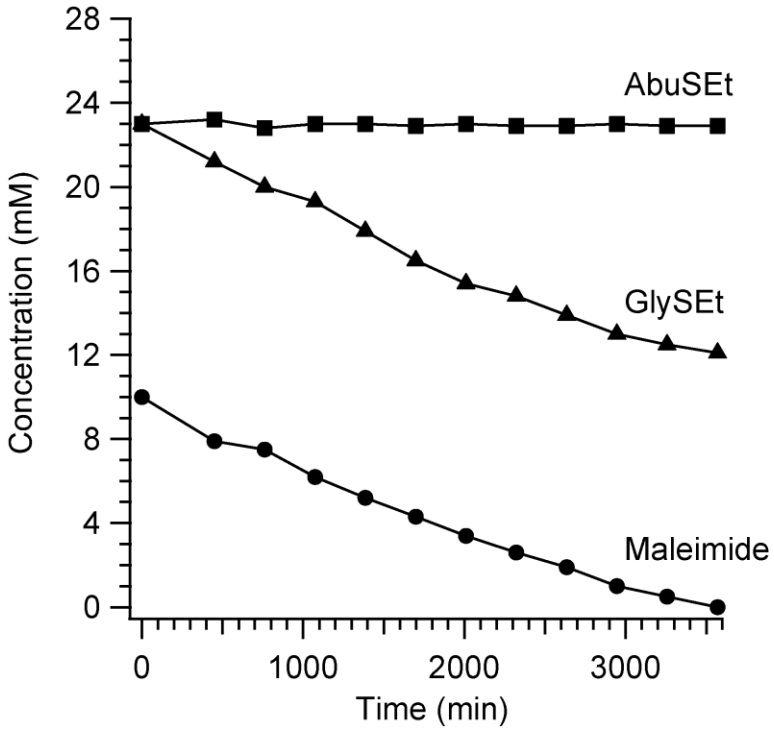

Figure S13. Plot from ^{1}H NMR kinetics experiments showing the loss of AbuSEt, GlySEt and maleimide over time. Concentration of reactants were the same as those used in the flow reactor: [AbuSEt] = 23 mM, [GlySEt] = 23 mM, [cystamine] = 46 mM, [sodium phosphate] = 500 mM, pH 7.5, 25 °C, D_2O. No change was observed in the concentration of AbuSEt before the maleimide was depleted (that is, when maleimide was at a concentration less than 0.1 mM).